Moving Axle Load From Multi-Span Continuous Bridge: Laboratory Study

Tommy H. T. Chan
Associate Professor
e-mail: cetommy@polyu.edu.hk

Demeke B. Ashebo

Department of Civil and Structural Engineering,
The Hong Kong Polytechnic University,
Hung Hom, Kowloon, Hong Kong, P. R. C.

Laboratory study on the identification of moving vehicle axle loads on a multi-span continuous bridge from the measured bending moment responses is presented. A bridge-vehicle system model was fabricated in the laboratory. The bridge was modeled as a three span continuous beam and the car was modeled as a vehicle model with two-axle loads. A number of strain gauges were adhered to the bottom surface of the beam to measure the bending moment responses. Using measured bending moment responses as an input, the corresponding inverse problem was solved to identify moving loads. The moving forces were identified when considering bending moment responses from all spans of the beam. In order to avoid the lower identification accuracy around the inner supports of continuous bridge and to improve the computation efficiency, the moving force identification from the target (one selected) span of the continuous bridge was studied. The rebuilt responses were reconstructed from the identified loads as a forward problem. To study the accuracy of the method the relative percentage errors were calculated with respect to the measured and the rebuilt bending moment responses. The rebuilt bending moment responses obtained from the identified forces are in good agreement with the measured bending moment responses. This indirectly shows that the method is capable of identifying moving loads on continuous supported bridges.
[DOI: 10.1115/1.2202154]

Keywords: moving axle load, bending moment responses, continuous bridge

1 Introduction

Highway bridges are mainly designed for passage of running trucks or heavy vehicles on top of them. Apart from other forces, in normal environmental and traffic conditions vehicle loads are the main loading component on bridge structures. In order to acquire efficient design, better maintenance, and management planning on bridge structures it is crucial to understand the behavior of bridge and dynamic axle load interactions.

In recent years methods have been developed to identify the dynamic component of the axle loads from bridge responses [1–5]. The methods used the measured bridge responses together with the vehicle and bridge parameters as an input and solve the inverse problem to approximate the dynamic forces induced by the vehicle on bridges. The above methods were proved to be effective in identifying moving forces and the accuracy of the methods was tested and found acceptable. However, the methods were applied on simply supported bridges. Zhu and Law [6] studied the identification of moving loads on a multi-span bridge. To validate their method and their numerical simulation they carried out experimental study by modeling the bridge as a simply supported beam in laboratory. Numbers of methods were developed to study the moving force identification problem on continuous bridge based on simulation studies [7,8].

In this paper a method is developed to identify moving forces on continuous bridges and the laboratory study of identification of dynamic loads on a multi-span continuous bridge is described. The bridge is modeled as a three span continuous beam made from steel and the vehicle is modeled as two axle car running on the top of the bridge. Moving forces induced by the two-axle car are identified from measured bending moment responses.

The accuracy of the identified time history of the bridge-vehicular interaction forces from continuous bridges is lower than that of the identified forces obtained from simple span bridges [9]. One reason for this is the lower identification accuracy around the supports of the continuous bridges. Apart from this, considering all the spans of the continuous bridge responses in the moving forces identification needs longer computation time. To improve the accuracy and the efficiency of moving force identification from continuous bridges, a method has been developed to identify the time history of the axle loads of a vehicle moving across a continuous bridge using the responses of a target span (one selected span) from the continuous bridge.

2 Vehicle Dynamic Load Identification

As shown in Fig. 1, the bridge superstructure is modeled as a multi-span continuous beam with a total span length L, constant flexural stiffness EI, constant mass per unit length ρ and viscous proportional damping C. The beam is assumed to be an Euler-Bernoulli beam, in which the effects of shear deformation and rotary inertia are not taken into account. The force on a bridge due to a moving vehicle is modeled as a point load acting through the axles of the car moving on the bridge from left to right at a constant speed. The equation of motion for a beam subject to an arbitrary external force is given by

$$\rho \frac{\partial^2 v(x,t)}{\partial t^2} + C \frac{\partial v(x,t)}{\partial t} + EI \frac{\partial^4 v(x,t)}{\partial x^4} = f(x,t) \qquad (1)$$

The initial and boundary conditions of Eq. (1) are given as

$$v(x,0) = f(x) \quad 0 \le x \le L$$

$$v_t(x,0) = g(x) \quad 0 \le x \le L$$

$$v(0,t) = v(l_r,t) = v(L,t) = 0 \quad t > 0$$
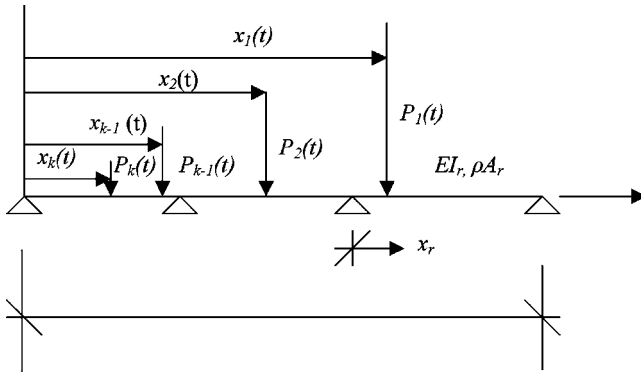
$$v_x(l_r,t) = v_x(0,t)$$

Fig. 1 Group of moving forces over the continuous beam

$$EI_r v_{xx}(l_r,t) = EI_{r+1} v_{xx}(0,t) \quad (2)$$

where the first two equations of Eq. (2) represent the initial conditions in which $f(x)$ and $g(x)$ are the displacement and velocity of the system, respectively, and L is the total length of the beam. The last three equations express the boundary conditions in which the displacement at each support point of the beam is zero and the slopes and bending moments at the common support of the two adjacent spans are equal, where l_r is the x coordinate at the last support point of span r.

Based on the modal superposition principle, the solution of Eq. (1) is expressed as

$$v(x,t) = \sum_{n=1}^{\infty} \Phi_n(x) q_n(t) \quad (3)$$

where $v(x,t)$ is the displacement of the system, $q_n(t)$ is the nth modal amplitude, and $\Phi_n(x)$ is the nth mode shape function of the beam. Once the two components on the right side of Eq. (3) are determined then the solution for the displacement is straightforward. The expression for $\Phi_n(x)$ for continuous boundary conditions of the beam at the support points is given in the Appendix. Substituting Eq. (3) into Eq. (1) and multiplying by Φ_n integrating the resultant equation with respect to x between 0 and L and then applying orthogonality conditions, the equation of motion in terms of the modal displacement $q_n(t)$ is given as

$$\frac{d^2 q_n}{dt^2}(t) + 2\xi_n \omega_n \frac{dq_n}{dt}(t) + \omega_n^2 q_n(t) = \frac{1}{M_n} \sum_{k=1}^{N_t} \Phi_n(x_k(t)) f(x,t)$$

$$(n = 1,2,\ldots,\infty) \quad (4)$$

where ω_n, ξ_n, and M_n are the modal frequency, damping ratio, and the modal mass of the nth mode, respectively. Where $f(x,t)$ is the forcing function [10]. For N_t number of axles it can be described in terms of the dynamic loads, $P_k(t)$

$$f(x,t) = \sum_{k=1}^{N_t} \delta(x - x_k(t)) P_k(t) \quad (5)$$

where $x_k(t)$ is the position of the kth force, and $\delta(t)$ the Dirac delta function. When $x = x_k(t)$ the forcing function is equal to the instantaneous value of the axle load $P_k(t)$. In all other locations where x is different from $x_k(t)$, the forcing function is zero.

Solving for $q_n(t)$ in a time domain method by convolution integral

$$q_n(t) = \frac{1}{M_n} \int_0^t h_n(t-\tau) P(\tau) d\tau \quad (6)$$

where $h_n(t-\tau)$ is the impulse response function and it is given by

$$h_n(t) = (1/\omega_n') e^{-\xi_n \omega_n t} \sin(\omega_n' t), \quad t \geq 0, \quad \text{and} \quad \omega_n' = \omega_n \sqrt{1 - \xi_n^2} \quad (7)$$

The dynamic deflection of the beam at point x and time t can be found as

$$v(x,t) = \sum_n \frac{\Phi_n(x)}{M_n} \int_0^t (1/\omega_n') e^{-\xi_n \omega_n(t-\tau)} \sin \omega_n'(t-\tau)$$

$$\times \sum_{k=1}^{N_t} P_k(t) \Phi_n(x_k(\tau)) d\tau \quad (8)$$

where $x_k(\tau)$ is the location of the moving force $P_k(t)$ at time t and N_t is the number of axles of the vehicle.

The bending moment of the beam at point x and time t is

$$m(x,t) = EI \frac{\partial^2 v(x,t)}{\partial x^2} \quad (9)$$

By substituting Eq. (8) into Eq. (9) and assuming that force $P_k(t)$ is a step function in a small time interval, then Eq. (9) can be written in discrete terms as

$$m(i) = -EI \sum_n \frac{\Phi_n''(x)}{M_n} \sum_{j=0}^i (1/\omega_n') e^{-\xi_n \omega_n \Delta t(i-j)} \sin \omega_n' \Delta t(i-j)$$

$$\times \sum_{k=1}^{N_t} P_k(j) \Phi_n(x_k(j))$$

$$i = 0,1,2,\ldots,N$$

$$j = 0,1,2,\ldots,NL \quad (10)$$

where N is the number of sample point, NL is the number of load step, Δt is sampling interval, $m(i)$ is bending moment at sample point i, ω_n is the nth natural frequency, ω_n' is the nth damped natural frequency, ξ_n is the nth damping ratio, and $\Phi_n(x)$ is the nth mode shape.

The bending moment responses from a target span r are given by

$$m_r(i) = -EI \sum_n \frac{\Phi_{nr}''(x_r)}{M_n} \sum_{j=0}^i (1/\omega_n') e^{-\xi_n \omega_n \Delta t(i-j)} \sin \omega_n' \Delta t(i-j)$$

$$\times \sum_{k=1}^{N_t} P_k(j) \Phi_{nr}(x_k(j))$$

$$i = 0,1,2,\ldots,N$$

$$j = 0,1,2,\ldots,NL \quad (11)$$

where $m_r(i)$ is the bending moment of the span under consideration, n is the mode number and Φ_{nr} is the nth mode shape of the span r.

Except the axle forces $P_k(j)$ all the other terms in the right side of Eqs. (10) and (11) are known and the bending moment on the left side of the equation can be obtained from measurement.

Equations (10) and (11) can then be arranged in matrix form

$$\mathbf{b} = \mathbf{A}\mathbf{x} \quad (12)$$

in which $\mathbf{b}$ represents the measured bending moment responses as indicated on the left side of Eqs. (10) and (11), $\mathbf{x}$ stands for the time varying moving force $P(t)$ to be identified, and $\mathbf{A}$ is a coefficient matrix which is associated with the system of the bridge deck and the vehicle as shown in the right side of Eqs. (10) and (11). The solution of Eq. (12) can be obtained by singular value decomposition (SVD) of the coefficient matrix $\mathbf{A}$. As shown by Yu and Chan [11] if A is real, the SVD of A is USV^T, where U is an
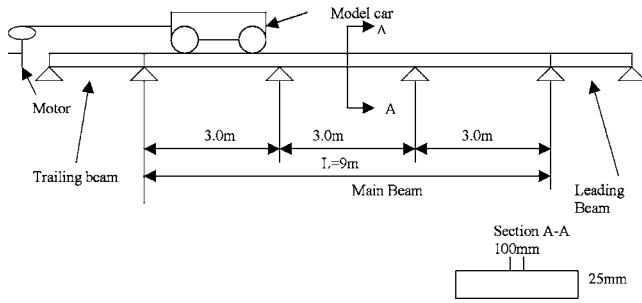
Fig. 2 Experimental setup

orthogonal $k \times k$ matrix, V is an orthogonal $n \times n$ matrix and S is a real diagonal $k \times n$ matrix in which the elements at the leading diagonal of the matrix are called the singular values of A. The least-squares solution vector x in Eq. (12) is given by

$$x = (VS^{-1}U^T)b \qquad (13)$$

where x is the force to be identified.

3 Laboratory Experiment

3.1 Laboratory Setup. A bridge-vehicle system model was fabricated in the laboratory. The bridge was modeled as a three span continuous supported beam and the car was modeled as a vehicle model with two-axle loads on the beam. The beam was chosen from a series of beam materials available in the market. It is made from mild steel with a density of 7850 kg/m^3 and a flexural stiffness $EI = 29.0$ KN/m^2. As shown in Fig. 2 the total length of the beam is 9 m, with 3 m for each span. The cross section of the beam is 100 mm by 25 mm. The leading and trailing beams were attached at both ends of the main beam, in which the leading beam was used for initiating the motion and the trailing beam was used for decelerating the vehicle. A U-shaped aluminum section was glued to the upper surface of the beams as a direction guide for the car. During the test the model car was pulled along the guide by a string wound around the drive wheel of an electric motor. Before deciding the weight and the axle spacing of the model vehicle, a weight and length scale study was carried out by comparing the weight and length ratios with real bridge and vehicle. A real bridge was assumed to be an equally spaced three-span reinforced concrete continuous bridge with a

total length of 90 m and the corresponding real vehicle was assumed to be a heavy truck with gross weight of 220 KN with an axle spacing of 5 m. A model car having two axles which were mounted on four rubber wheels was designed. Based on the length ratio test the axle spacing was found to be 0.5 m. On the basis of the weight ratio scale the mass of the model car and each axle were estimated. The first fundamental frequency of the model bridge found from measurement was 7 Hz. Before the actual test it was found that the gross static mass of the car was 14.5 kg in which the front axle and the rear axle weighed 5.2 and 9.3 kgs, respectively.

3.2 Sensors Arrangement and Data Acquisition. Eleven strain gauges were mounted at the bottom of the main beam to measure the bending moment responses. From these five were on the middle span of the beam and the rest were on the outer two spans, three on each of the spans. Fourteen photoelectric sensors were installed at every 0.75 m gap. These photoelectric sensors had two main functions; the first was to measure the speed of the running vehicle at the top of the beam and the second was to serve as triggering point. The installations of these photoelectric sensors were arranged in such a way as to show the origin points of every span (i.e., out of 14 photoelectric sensors four were installed just ahead of each of the four support points of the beam). Therefore, due to this arrangement of photoelectric sensors in the data analysis stage, it was possible to get the required data for a specific span. The arrangement of the sensors on the main beam is shown in Fig. 3. To relate the voltage reading of the strain gauges with bending moments, a system calibration was carried out before the actual testing program by adding known quantity of masses at the middle points of each of the three spans. The software LABVIEW from National Instruments was used for data acquisition and analysis. The data were recorded through 12 channels, in which the first channel was for the data input from photoelectric sensors and the other 11 were for data reading from strain gauges. Figure 4 shows the output of photoelectric sensors from channel 0 and the measured strain in terms volt form channel 6 (midpoint of the middle span). The data were acquired in 1000 Hz sampling frequency, which is higher than the practical demands. The data sequences were sampled again to form a new data sequence at lower sampling frequency. Before using the data for force identification study, from MATLAB tool box the Butterworth digital filter with low pass characteristics of 40 Hz cutoff frequency was implemented with a second-order system to carry out filtering.
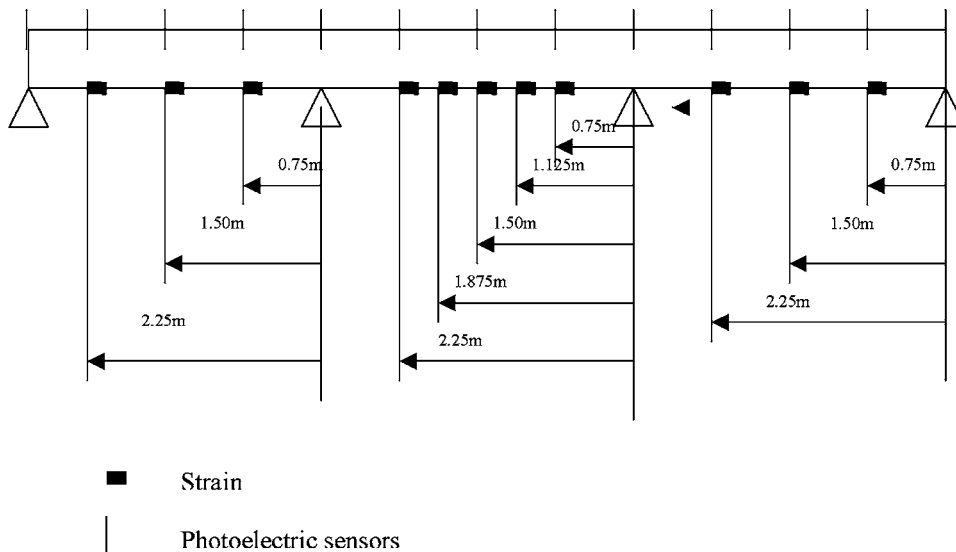

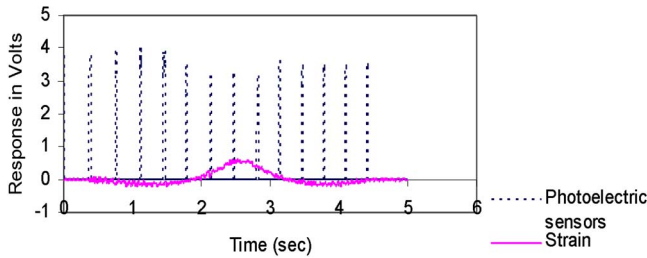**Fig. 3 Sensors arrangement on the main beam**

Fig. 4 Output of photoelectric sensors and strain gauge

3.3 Moving Force Identification. Identifications of moving force have been carried out from the recorded measured bending moment responses in a time gap between the first axle crossing the first entry point of the first span and the second axle of the vehicle crossing the last point of the third span. In addition to this, the measured bending moment responses obtained from the middle span were used to validate the moving force identification from a target (one selected) span of a continuous beam model. For both cases the measured speed was found to be 2.25 m/s. In order to study the accuracy of the method the rebuilt responses were reconstructed from the identified loads. Then the relative percentage errors (RPE) were computed with respect to the measured bending moment and the rebuilt bending moment responses using Eq. (14)

$$\text{RPE} = \frac{\sum_{i=1}^{N} |\text{Re } s_{\text{measured}}(i) - \text{Re } s_{\text{rebuilt}}(i)|}{\sum_{i=1}^{N} |\text{Re } s_{\text{measured}}(i)|} \tag{14}$$

where N is the number of sampling point, RPE is the relative percentage error, Re s_{measured} and Re s_{rebuilt} are the measured and
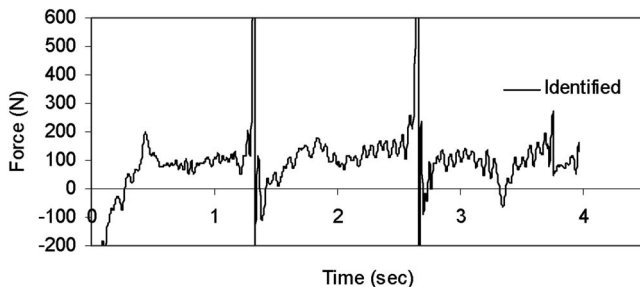
Front axle
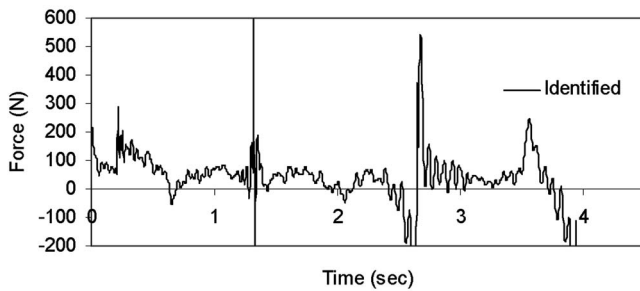
Rear axle
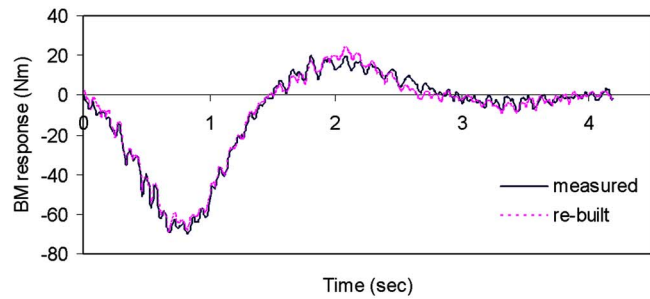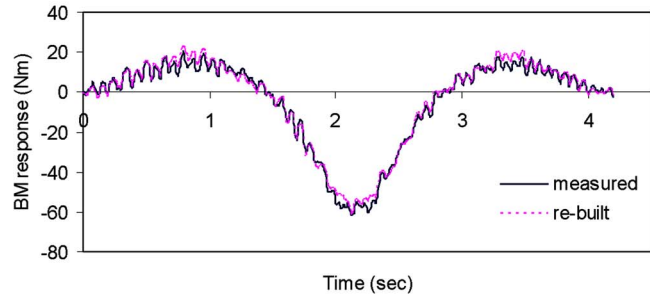

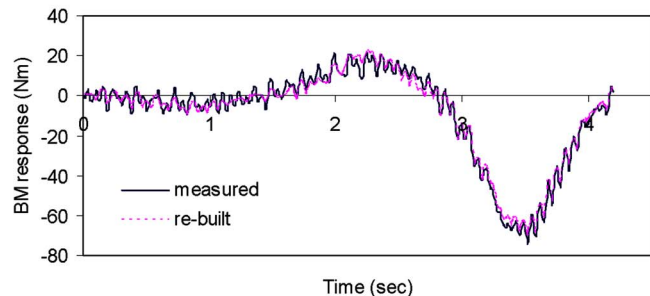Fig. 5 Identified axle loads for multi-span continuous case

Fig. 6 The measured and rebuilt bending moment responses for continuous beam case at midpoint of each span

rebuilt responses, respectively.

3.3.1 Results for Multi-Span Continuous Beam Case. Due to the limited memory capacity of the computer, only measured bending moment responses obtained from seven measuring locations were used in the moving force identification for continuous beam case in which two were from each of the outer spans and three from the middle span. The sampling frequency was taken to be 166 Hz. The identified moving forces for continuous beam case are shown in Fig. 5. As it can be seen from Fig. 5, the identified forces from the continuous beam model are affected at the vicinity of the supports which is also in good agreement with the theoretical results reported by Chan and Ashebo [8]. The accuracy of identified forces is also affected at the moments of entry of the front axle to the main beam and exit of the rear axle from the main beam. For this reason the accuracy of the identified forces is more affected at the outer spans than the middle span. The relative percentage error (RPE) values between the measured and the rebuilt bending moment responses are given in Table 1 for each strain gauge and it can be noticed that the calculated value of RPE of middle span is less than that of the two outer spans. This indirectly shows that, the accuracy of the identified forces in middle span is better than that of the two outer spans. The mea-

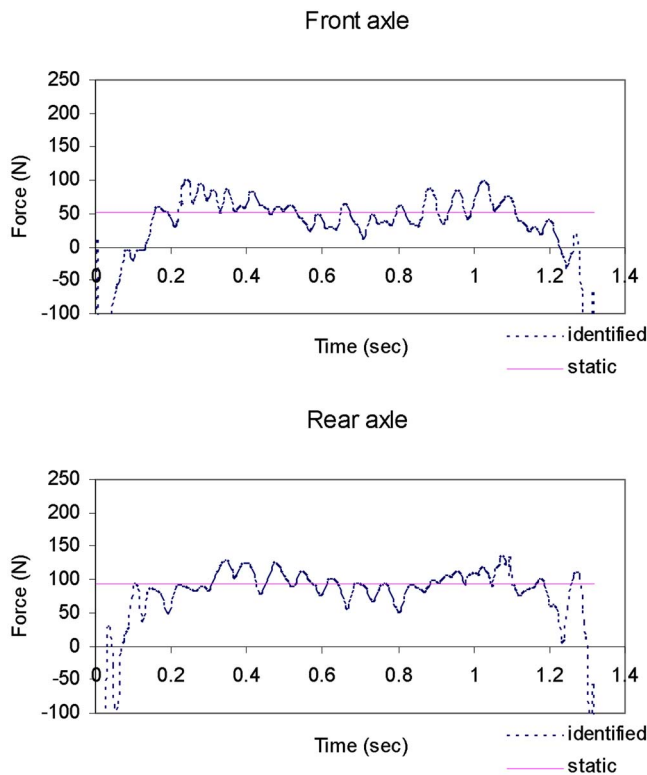**Table 1 The relative percentage error (RPE) values for continuous beam**

Channel no.	2	3	5	6	7	9	10
RPE (%)	12.12	13.99	9.11	10.11	12.35	18.38	14.13

Table 2 The relative percentage error (RPE) values for middle span

Channel no.	4	5	6	7	8
RPE (%)	7.68	4.83	4.27	6.10	11.89

Fig. 8 The measured and rebuilt bending moment responses at midpoint of target span (for middle span case)

sured and the rebuilt bending moment responses for continuous beam case at the midpoint of each span are given in Fig. 6.

3.3.2 Results for Target Span Case. For the case of moving force identification from the target span, the middle span is selected as a target span to study the effectiveness of the method. Measured bending moment responses from five measuring locations in the middle span are used and the sampling frequency is taken to be 333 Hz. The identified dynamic axle loads are shown in Fig. 7. In addition, the average of the middle 80% of the identified dynamic axle loads are computed to approximate the static load of the axles which are very close to the corresponding measured static axle forces. As it can be noticed from Fig. 7, the accuracy of the identified forces is better than that of the continuous beam case. The measured and rebuilt bending moment responses at midpoint of the middle span for this case are given in Fig. 8. The relative percentage error (RPE) between the measured and the rebuilt bending moment responses are given in Table 2 for all of five strain gauges. As can be noticed from the table, the RPE values for identification from the target span (middle span) case are less than that of the continuous beam case. This shows that,

apart from other advantages, using the responses of only one span of continuous beam for moving force identification gives better accuracy than using all spans of the continuous beam. The other merits of using this method are (a) it needs less computation time and (b) it needs sensors installation only at the span under consideration. This can save a lot of time during sensors installation especially in actual field tests.

4 Conclusions

The method for moving force identification for continuous bridges is developed and validated by laboratory study. The bending moment responses have been measured as an input for the inverse problem for moving force identification. The results obtained from the analysis of the laboratory study show that it is possible to identify moving vehicle forces from measured bending moment responses on a continuous bridge by the method developed. Identification of moving forces from both the continuous beam and target span cases are carried out, and the relative percentage errors (RPE) between the measured and the rebuilt bending moment responses are computed in order to study the accuracy of the method indirectly. From the results obtained from identified forces and the RPE study the method can identify moving forces in acceptable accuracy; however, the accuracy of the method is affected at the vicinity of supports. In addition to this, it is found that using all spans of the continuous bridge needs long computation time and large computer memory. In order to minimize this problem, the moving force identification from a target span has been introduced in which better identification accuracy is attained. Moreover, while carrying out the case study, it was found that moving force identification from the target span of the continuous beam case needs less computation time than that of the continuous beam case.

Fig. 7 Identified and static forces for target (middle) span case

Nomenclature

A_r = cross-sectional area of the beam at span r
C = viscous damping of beam
EI = flexural stiffness
EI_r = flexural stiffness of the span r
I = second moment of area
L = total length of beam
l_r = the x coordinate at the last support point of span r
m = bending moment
m_r = bending moment of span r
Mn = modal mass of nth mode
n = mode number
N = number of sample data point

$$D_{n,1} = 0 \qquad (A5)$$

For the inner spans

$$B_{n,r+1} = -\frac{(\lambda_{n,r})^2}{(\lambda_{n,r+1})^2} \times (I_r/I_{r+1}) \times (-A_{n,r} \sin \lambda_{n,r}L_r - B_{n,r} \cos \lambda_{n,r}L_r$$

$$+ C_{n,r} \sinh \lambda_{n,r}L_r + D_{n,r} \cosh \lambda_{n,r}L_r)/2$$

$$D_{n,r+1} = -B_{n,r+1}$$

$$A_{n,r+1} = -B_{n,r+1}(\cos \lambda_{n,r+1}L_{r+1} - \cosh \lambda_{n,r+1}L_{r+1}) - \frac{\lambda_{n,r}}{\lambda_{n,r+1}}$$

$$\times (A_{n,r} \cos \lambda_{n,r}L_r - B_{n,r} \sin \lambda_{n,r}L_r + C_{n,r} \cosh \lambda_{n,r}L_r$$

$$+ D_{n,r} \sinh \lambda_{n,r}L_r) \times \frac{\sinh \lambda_{n,r+1}L_{r+1}}{\sin \lambda_{n,r+1}L_{r+1} - \sinh \lambda_{n,r+1}L_{r+1}}$$

$$C_{n,r+1} = \frac{\lambda_{n,r}}{\lambda_{n,r+1}} \times (A_{n,r} \cos \lambda_{n,r}L_r - B_{n,r} \sin \lambda_{n,r}L_r + C_{n,r} \cosh \lambda_{n,r}L_r$$

$$+ D_{n,r} \sinh \lambda_{n,r}L_r) - A_{n,r+1}$$

For the last span

$$B_{n,r+1} = -\frac{(\lambda_{n,r})^2}{(\lambda_{n,r+1})^2} \times (I_r/I_{r+1}) \times (-A_{n,r} \sin \lambda_{n,r}L_r - B_{n,r} \cos \lambda_{n,r}L_r$$

$$+ C_{n,r} \sinh \lambda_{n,r}L_r + D_{n,r} \cosh \lambda_{n,r}L_r)/2$$

$$D_{n,r+1} = -B_{n,r+1}$$

$$C_{n,r+1} = B_{n,r+1}(\cosh \lambda_{n,r+1}L_{r+1}/\sinh \lambda_{n,r+1}L_{r+1})$$

$$A_{n,r+1} = \frac{\lambda_{n,r}}{\lambda_{n,r+1}} \times (A_{n,r} \cos \lambda_{n,r}L_r - B_{n,r} \sin \lambda_{n,r}L_r + C_{n,r} \cosh \lambda_{n,r}L_r$$

$$+ D_{n,r} \sinh \lambda_{n,r}L_r) - C_{n,r+1}$$

where $n = 1, 2 \ldots$, total number of mode

$$r = 1, 2, \ldots, \text{ total number of span}$$

I_r is the second moment of area of the span r

L_r is length of span r

Nomenclature

$$
\begin{aligned}
NL &= \text{Number of load point} \\
N_t &= \text{the number of axles of the vehicle} \\
P(t) &= \text{time varying concentrated force} \\
q_n &= n\text{th modal amplitude} \\
v &= \text{displacement of the beam} \\
\rho &= \text{mass per unit length of beam} \\
\omega_n &= n\text{th modal frequency} \\
\omega_n' &= \text{damped } n\text{th modal frequency} \\
x_k(t) &= \text{position axle force at time } t \\
\xi_n &= \text{damping ratio of } n\text{th mode} \\
\Phi_n &= \text{mode shape function of } n\text{th mode} \\
\mathbf{x} &= \text{force vector} \\
\mathbf{m} &= \text{bending moment vector}
\end{aligned}
$$

Appendix: Free Vibration of Continuous Beam

While dealing with the free vibration of an Euler-Bernoulli beam, the right side of Eq. (1) of equation of motion transforms to zero and is given by

$$\rho \frac{\partial^2 v(x,t)}{\partial t^2} + C \frac{\partial v(x,t)}{\partial t} + EI \frac{\partial^4 v(x,t)}{\partial x^4} = 0 \qquad (A1)$$

Substituting the modal expansion of Eq. (3) into Eq. (A1) and ignoring the small damping term, then by separation of variable the equation of motion transforms to the fourth-order ordinary differential equation

$$\frac{d^4 \Phi_n}{dx^4}(x) - \lambda_n^4 \Phi_n(x) = 0 \qquad (A2)$$

For the rth span of the general case of a continuous beam, the solution of Eq. (A2) is given by

$$\Phi_{nr}(x_r) = A_{nr} \sin(\lambda_{nr}x_r) + B_{nr} \cos(\lambda_{nr}x_r) + C_{nr} \sinh(\lambda_{nr}x_r)$$

$$+ D_{nr} \cosh(\lambda_{nr}x_r) \qquad (A3)$$

where $\Phi_{nr}(x_r)$ is the nth modal shape function of the rth span, x_r is the distance from the first support of the span under consideration, and λ_{nr} is the eigenvalue of the system to be obtained from

$$\lambda_{nr} = \sqrt[4]{\frac{\rho_r \omega_n^2}{EI_r}} \qquad (A4)$$

where ρ_r and EI_r are mass per unit length and the stiffness of the rth span, respectively, and ω_n is the nth natural frequency of the beam.

The arbitrary constants A_{nr}, B_{nr}, C_{nr}, and D_{nr} in Eq. (A3) can be determined from substituting the boundary and initial conditions of Eq. (2) into Eq. (A3). The calculation of the eigenfunctions is just a matter of substituting the appropriate boundary conditions in Eq. (A3)

Equation (A3) applies to spans with arbitrary boundary conditions at the outer and inner supports. In this paper it is assumed that the outer two end support conditions are simply supported and the beam is continuous over the inner supports.

After substituting the boundary conditions of Eq. (2) into Eq. (A3), the constants A_{nr}, B_{nr}, C_{nr}, and D_{nr} can be obtained from the following expressions which are straightforward and easy for computer programming:

For the first span

$$A_{n,1} = 1$$

$$B_{n,1} = 0$$

$$C_{n,1} = -\sin \lambda_{n1}L_1/\sinh \lambda_{n1}L_1$$

References

[1] Chan, T. H. T., and O'Connor, C., 1990, "Wheel Loads From Highway Bridge Strains—Field Studies," J. Struct. Eng., **116**, pp. 1751–1771.

[2] Chan, T. H. T., Law, S. S., Yung, T. H., and Yuan, X. R., 1999, "An Interpretive Method for Moving Force Identification," J. Sound Vib., **219**(3), pp. 503–524.

[3] Law, S. S., Chan, T. H. T., and Zeng, Q. H., 1997, "Moving Force Identification—Time Domain Method," J. Sound Vib., **201**(1), pp. 1–22.

[4] Law, S. S., Chan, T. H. T., and Zeng, Q. H., 1999, "Moving Force Identification—A Frequency Time Domains Approach," ASME J. Dyn. Syst., Meas., Control, **121**(3), pp. 394–401.

[5] Chan, T. H. T., Law, S. S., and Yung, T. H., 2000, "Moving Force Identification Using an Existing Prestressed Concrete Bridge," Eng. Struct., **22**(10), pp. 1261–1270.

[6] Zhu, X. Q., and Law, S. S., 2001, "Orthogonal Function in Moving Loads Identification on a Multi-Span Bridge," J. Sound Vib., **245**, pp. 239–345.

[7] Jiang, R. J., Au, F. T. K., and Cheung, Y. K., 2004, "Identification of Vehicles Moving on Continuous Bridges," J. Sound Vib., **274**(3–5), pp. 1045–1063.

[8] Au, F. T. K., Jiang, R. J., and Cheung, Y. K., 2004, "Parameter Identification of Vehicles Moving on Continuous Bridges," J. Sound Vib., **269**(1–2), pp. 91–111.

[9] Chan, T. H. T., and Ashebo, D. B., 2006, "Theoretical Study of Moving Force Identification on Continuous Bridges," J. Sound Vib. (in press).

[10] Cebon, D., 1999, *Hand Book of Vehicle-Road Interaction*, Sweets & Zeitlinger.

[11] Yu, L., and Chan, T. H. T., 2003, "Moving Force Identification Based on the Frequency-Time Domain Method," J. Sound Vib., **261**(2), pp. 329–349.